Study on Microstructure and Properties of TIG Welded Joint of TC2 Titanium Alloy and Quality Inspection

JIANG Jian[1], *QI Lichun*[2], *ZHANG Mingjie*[2], *CHEN Wenhua*[1], *SHEN Yifu*[1*]

1. College of Materials Science and Technology, Nanjing University of Aeronautics and Astronautics, Nanjing 211106, P.R. China;

2. Institute of Titanium Alloy, Beijing Institute of Aeronautical Materials, Beijing 100095, P.R. China

(Received 18 November 2020; revised 31 January 2021; accepted 3 June 2021)

Abstract: TIG welding experiments of TC2 titanium alloy sheet was carried out, and the well-formed weld was obtained. After welding process, the cross-section microstructure, mechanical properties, fracture morphology and quality inspection of the joint were studied. The results show that the microstructure of the weld consists of a large number of acicular α′ and β block. The microhardness curve shows that the microhardness value in the fusion zone (FZ) of the joint is significantly higher than that in the heat affected zone (HAZ) and the base metal (BM), and the microhardness of the base metal is the lowest. The tensile strength of the joint is equivalent to that of the base metal, and the fracture morphology shows that the fracture mechanism of the joint is mixed ductile-brittle fracture mode. The weld quality is excellent through chemical inspection, penetrant inspection and X-ray inspection.

Key words: TC2 titanium alloy; TIG welding; microstructure; mechanical properties; quality inspection

CLC number: TG146; TG668 **Document code**: A **Article ID**: 1005-1120(2021)03-0484-08

0 Introduction

Titanium and titanium alloys are widely used in aerospace, chemical parts, medical engineering and other civil and military industries due to their excellent performance characteristics[1-4]. TC2 belongs to α + β type dual phase titanium alloy. It has good comprehensive properties, excellent microstructure stability, good toughness, plasticity and high-temperature deformation properties. It has been widely used in aviation key components and aircraft structural parts, mainly used in manufacturing compressor disk, blade, annular parts and fasteners of aircraft engine[5-10]. However, when the processing temperature is higher than 500 ℃, the titanium surface is easy to absorb oxygen, nitrogen, hydrogen and other gases. It is titanium that is colored by gas absorption, resulting in increased brittleness and hardness. Therefore, in order to minimize these problems, it is necessary to introduce appropriate shielding medium to cover the local welding area[11-13]. Tungsten inert gas (TIG) welding has many advantages for joining titanium alloy, such as lower cost, easing to realize automation and arc stabilization[14-15]. At present, the research on TIG welding of TC2 titanium alloy is relatively less. This paper studies the microstructure and properties of TC2 titanium alloy argon arc welding joint, analyzes its fracture morphology, and uses a variety of detection methods to determine the weld quality, and obtains the TIG welding joint with excellent performance.

*Corresponding author, E-mail address: yfshen_nuaa@hotmail.com.

How to cite this article: JIANG Jian, QI Lichun, ZHANG Mingjie, et al. Study on microstructure and properties of TIG welded joint of TC2 titanium alloy and quality inspection[J]. Transactions of Nanjing University of Aeronautics and Astronautics, XXXX, 38(3): 484-491.

http://dx.doi.org/10.16356/j.1005-1120.2021.03.012

1 Materials and Methods

In this experiment, TC2 titanium alloy plate was rolled. The joint form of the test piece was butt joint. The size of the test piece was 300 mm×100 mm×2.0 mm. The chemical composition of TC2 plate is shown in Table 1. Before welding, the titanium alloy sample and its surrounding area were pickled to remove the dense oxide film and impurities on the surface of the sample. The acid washing solution was 35% HNO_3 + 5% HF + 60% H_2O. After pickling, it was washed with clean water, and then wiped with absolute ethanol, and it was dried for subsequent use. The type of equipment used in the test is PANDJIRIS. In order to prevent oxidation, the requirement of gas protection is very high in the welding process of titanium alloy, and strict control measures must be taken. During welding, three channels (main nozzle, support cover and back) argon protection are adopted. The flow rate of protective gas is 15—20 L/min, and the diameter of tungsten electrode is 2.4 mm. The test parameters of welding process optimization are shown in Table 2. After welding, the argon arc welding joint passes Sans cmt-5105 electronic universal tensile testing machine, and the performance test is conducted according to GB/2651—2008 standard. The test temperature is room temperature, and the average value of the same parameter sample is taken for three times. The tensile specimen form of welded joint is shown in Fig.1. The cross-section microhardness of TIG welded joint was tested and analyzed by HXS-1000A microhardness tester. The load was 200 g, and the pressure was maintained for 15 s before unloading. The metallographic samples were taken perpendicular to the weld direction, and the cross-section was corroded by Keller reagent. The macrostructure of the samples was analyzed by using the orca binocular XTL-2600 microscope. The microstructure of argon arc welding joint and fracture surface was analyzed by scanning electron microscope (SEM).

Table 1 Chemical compositions of TC2 alloy substrate

%

Element	H	N	C	Si	Fe	Mn	B	Al	Ti
Weight percentage	0.06	0.15	0.012	0.05	0.08	1.43	0.22	4.09	Bal.

Table 2 TIG welding process parameters

Welding speed/(mm•s^{-1})	Welding current/A	Arc voltage/V
5.9	150—170	9.0—9.5

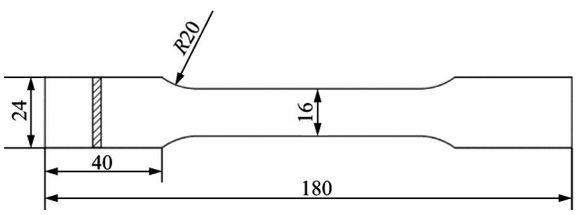

Fig.1 Schematic diagram of joint tensile specimen

The quality of the joint was analyzed by means of penetrant inspection, X-ray flaw detection and chemical inspection. The penetrant inspection was used to detect the surface defects of TIG joints. First, evenly spray the colorant on the weld surface and leave it for 10—15 min until the colorant fully penetrates into the weld. Then spray the imaging agent on the surface and leave it for 15 min to complete the penetrant test. In order to characterize the internal defects of the joint, X-ray flaw detection was performed by Bossle circular X-ray machine, Italy. The focus size is 0.4 mm × 4.0 mm, tube head diameter is 100 mm, and rod anode diameter is 33 mm. Also, the focal length is 800 mm, the tube voltage is 85—95 kV, the tube current is 8 mA, and the exposure time is 2 min. Chemical inspection was applied to determine the content of N, H and O of TIG joint. When analyzing the sample, the sample is weighed and put into the sample port, and then washed with carrier gas to prevent the atmosphere (including oxygen and nitrogen) from entering the furnace system. The graphite crucible is degassed in the pulse furnace to minimize the pollution. After stabilization, the sample falls into the crucible and melts. The oxygen in the sample reacts

with the carbon in the graphite crucible to form carbon monoxide. Nitrogen and hydrogen are released in the form of simple substance. The carrier gas and sample gas pass through the dust filter and then enter the copper oxide catalytic furnace to oxidize carbon monoxide into carbon dioxide. Carbon dioxide enters the infrared cell to determine the oxygen content. The measured gas is introduced into the chemical reagent tube. At this time, carbon dioxide and water are removed by the chemical reagent, and nitrogen is determined through the thermal conductivity detection cell. When measuring hydrogen, the carrier gas is replaced by nitrogen, and the sample gas passes through Schutz reagent instead of copper oxide catalyst.

(a) Weld surface

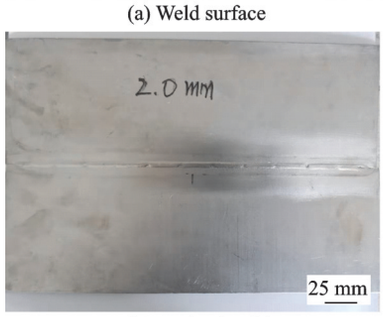

(b) Back of weld

Fig.2 Weld appearance

2 Results and Discussion

2.1 Inspection and analysis of joint quality

Fig.2 shows the appearance of weld surface. Under strict argon protection, the weld does not appear oxidation. However, due to the excessive heat input, the weld surface overheats and burns, but it does not affect the overall performance of the joint. The surface of the weld shows fish scale pattern, which is smooth, uniform and delicate. And there are no defects such as incomplete penetration, undercut, inclusion, arc pit, burn through, weld bead and pit.

The chemical properties of titanium are very active. At high temperature, the diffusion rate of oxygen in titanium increases and brittle layer is formed. The more oxygen content in titanium, the more serious the embrittlement. Hydrogen is easy to form interstitial solid solution TiH_2 in titanium, which acts as the source of microcracks in the joint and reduces the ductility and toughness of the joint. Nitrogen and titanium are strongly combined to form tin at high temperature, which causes serious lattice distortion and decreases the plasticity and toughness of the joint. Therefore, it is of great significance to control the content of oxygen, nitrogen and hydrogen in the joint. During the whole welding process, three channels (main nozzle, supporting cover and back side) of argon are used for protection. Table 3 shows the inspection results of chemical method. The allowable oxygen content in the weld is not more than 0.1%, and the nitrogen and hydrogen content are not more than 0.01%. The chemical analysis results meet the requirements and are qualified.

Table 3 Results of chemical analysis %

Sample	Element (Weight percentage)		
	O	N	H
1	0.09	0.009	0.004 1
2	0.09	0.008	0.003 9
3	0.09	0.008	0.003 2

Penetrant inspection is carried out on the surface and back of the weld. Fig.3 shows the image of penetrant inspection. First, the surface of the weld is evenly sprayed with the colorant and placed for 10—15 min until the dye is fully penetrated into the weld. Then spray the imaging agent on the surface and place it for 15 min. The penetrant inspection is completed. Through penetrant inspection, there are no surface cracks, pitting corrosion, incomplete fusion and other defects.

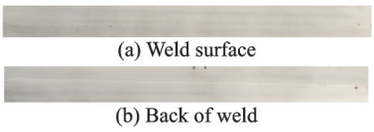

Fig.3 Penetrant inspection of joint surface morphology

In order to characterize the internal defects of the joint, X-ray inspection was carried out on the joint, and the inspection method was 100% inspection. According to the radiographic inspection, no over standard defects were found in the weld joint and heat affected zone (HAZ) of the argon arc welding sample. The internal porosity, shrinkage cavity, crack and spatter all meet the relevant acceptance requirements of Q/J11-3059—2002 standard. The X-ray examination image is shown in Fig.4.

Fig.4 X-ray examination negative image of TIG welding joint

2.2 Microstructure analysis of TIG welding joint

The microstructure of TC2 base metal (BM) is shown in Fig.5. The microstructure of the alloy at room temperature is mainly equiaxed structure composed of primary α phase and β phase, which has good plasticity and strength at room temperature. Fig.6 shows the appearance of TIG welding joint, and the joint has obvious zoning phenomenon, which is mainly composed of base metal, heat affected zone and fusion zone (FZ). TC2 titanium alloy has high melting point, large heat capacity and poor thermal conductivity. The high temperature residence time is long due to the large welding heat input. Therefore, the fusion zone and heat affected zone of TC2 titanium alloy are large, with the sizes of 5.2 mm and 4.2 mm, respectively.

Fig.7 shows the SEM of a, b and c in Fig.6. As shown in Fig.7(a), the grains in the fusion zone are relatively coarse, and the microstructure of the grains mainly consists of acicular martensite. During welding, due to the rapid cooling of the fusion zone from the β phase zone, α phase has no time to precipitate from the blocky β phase, and the atoms in β phase will migrate in a short range and transform into α′ martensite with dense hexagonal lattice. The acicular α′ martensite nucleates and grows in original β grain interior and β grain boundary at the same

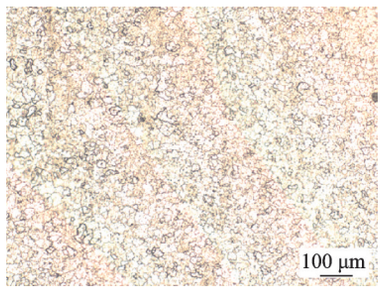

Fig.5 Microstructure of TC2 titanium alloy

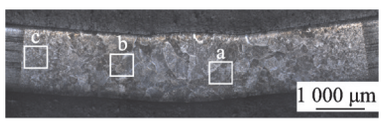

Fig.6 Macrostructure of TC2 TIG welding joint

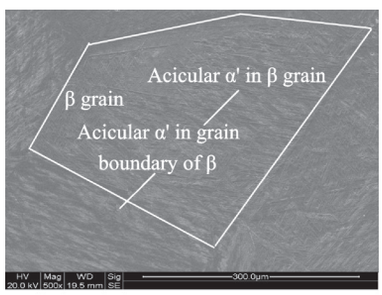

(a) Microstructure of FZ

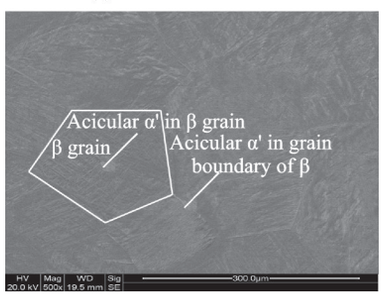

(b) Microstructure of HAZ

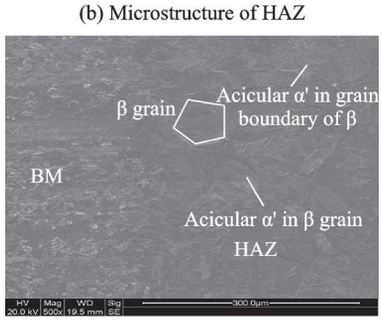

(c) Microstructure of HAZ/BM interface

Fig.7 Microstructure of TIG welding joint

time. Firstly, a number of parallel primary α′ martensites are formed and grow through the whole grain boundary, which are divided by the original β grain boundary. Then, relatively fine secondary acicular α′ martensites are formed, it is mainly distributed in the β grain. In the TIG welding process, owing to gradient distribution of the temperature field with the weld as the symmetry center, the heterogeneous HAZ structure was formed. As shown in Figs.7(b) and (c), there are obvious differences in the microstructure between the HAZ near the fusion zone and the base metal. Fig.7(b) shows the structure of HAZ close to the fusion line. The structure of HAZ is mainly composed of primary α phase, β transformation phase and acicular martensite, but acicular martensite is less than that of fusion zone. The highest temperature of HAZ is lower than that of the fusion zone, and the cooling rate is lower than that of the fusion zone, so the acicular α′ martensite is less and finer. However, in the heat affected zone (Fig.7(c)) close to the base metal, the grain coarsening is not obvious due to its lower welding temperature, and the grains are equiaxed, and the acicular α′ martensite could hardly be seen in HAZ near the base metal. It is obviously detected in Fig.7 that the grain size decreases with the increase of distance from the weld center.

Fig.8 shows the cooling rate of each area of the joint. The high heat input in the center of TIG weld (area a) and the difficulty in heat dissipation during the welding process leads to the serious coarsening of the grain in the weld center, which is harmful to the mechanical properties of the joint. Because of the high welding temperature, even if slow the heat dissipation, the cooling rate is fast, and a large amount of acicular α′ martensite is formed in the grain interior and grain boundary. Due to the solid solution and dispersion strengthening effect, the mechanical properties of TIG joint are greatly improved. In the heat affected zone (zone c) near the base metal, the welding temperature is not high and the heat dissipation is fast, the recrystallized grains formed in the zone do not grow in time, so the grains are relatively small. Owing to the low temperature in this region, there is no acicular α′ martensite in the cooling process. The grain size of HAZ near the weld zone (zone b) is between the zone a and zone c.

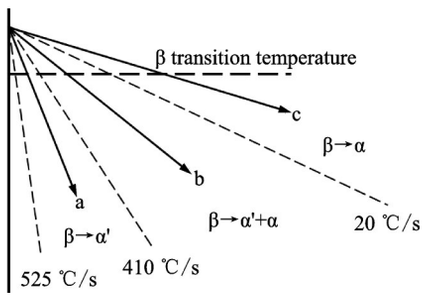

Fig.8 Schematic diagram of cooling rate in different zones of TC2 by TIG welding

2.3 Analysis of mechanical properties and fracture morphology

2.3.1 Microhardness

In order to understand the difference of mechanical properties in different regions of argon arc welding joint more intuitively, the microhardness of the joint was tested. The microhardness curve of TIG welding joint is shown in Fig.9. It can be seen from the curve that the microhardness in the fusion zone of the joint is significantly greater than that in the heat affected zone and base metal, and the microhardness of the base metal is the lowest. The microhardness of the base metal is 270—285 $HV_{0.2}$, the microhardness of the fusion zone is 415—440 $HV_{0.2}$, and the microhardness of the heat affected zone is between that of BM and FZ. This is mainly due to the rapid cooling rate of the fusion zone during cooling process, and a large amount of acicular α′ martensite is formed in the grain, which greatly improves the strength and deformation resistance of the fusion zone. However, the low welding temperature and short high temperature residence time in HAZ result in low cooling rate and less acicular α′ martensite. With the increase of distance from the weld center, the amount of acicular α′ martensite decreases gradually, so the microhardness of HAZ decreases significantly with the increase of distance.

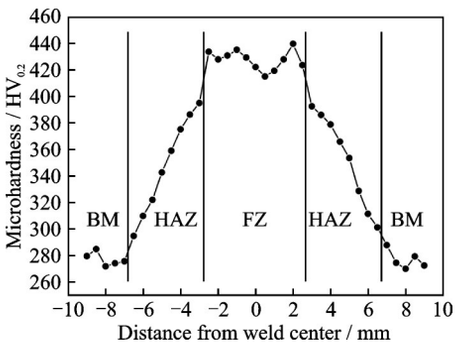

Fig.9 Microhardness curve of TIG welding joint

2.3.2 Tensile property

The tensile properties of TIG welded joints were tested, and the results are shown in Table 4. The fracture position of TIG welded joints are showed in Fig.10. The fracture position of sample 1 is the base metal, and the tensile strength is 844 MPa, while that of samples 2 and 3 is 841 MPa and 843 MPa, respectively. The results show that the tensile strength of joint is equivalent to that of the base metal. Even if the grains in the weld zone are coarse, the high-strength weld can be obtained after welding. This is mainly due to the formation of a large amount of acicular martensite in the welding process, which greatly improves the tensile strength of the weld owing to the appearance of solid solution strengthening effect and dispersion strengthening effect. It eliminates the joint strength reduction caused by coarse grains in the weld area to a certain extent. The tensile fracture morphology of sample 2 is shown in Fig. 11. It can be seen from the SEM in Fig.11(a), the tensile fracture is a mixed ductile-brittle fracture mode. And obvious fluvial pattern is found in Fig.11(a). Figs.11(b) and (c) are enlarged views of local regions 1 and 2, respectively. Area 1 presented quasi-cleavage fracture with mixed cleavage and dimple features. In the enlarged SEM images of area 2, the fracture surface exhibited ductile fracture, characterized by dimples with a shallow depth. As shown in Fig.11(c), there are obvious ductile fracture characteristics, and there are also brittle fractures in the fracture surface of tensile samples, demonstrating that the fracture mode of the TIG joint was mixed fracture. Because of the non-uniformity of microstructure and mechanical properties, the HAZ is the weakest area of the whole joint, where the fracture often occurs. However, its strength is still equivalent to that of the base metal. In a word, the fracture morphology exhibited cleavage facet and dimples, so the fracture is a mixed ductile-brittle fracture mode.

Table 4 Tensile properties of TIG welded joint

Sample	Tensile strength/MPa	Yield strength/MPa	Fracture location
1	844	708.3	Base metal
2	841	692.7	Weld joint
3	843	697.1	Weld joint

Fig.10 Fracture position of tensile specimen

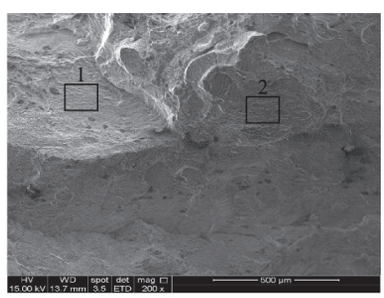

(a) Macroscopic fracture morphology

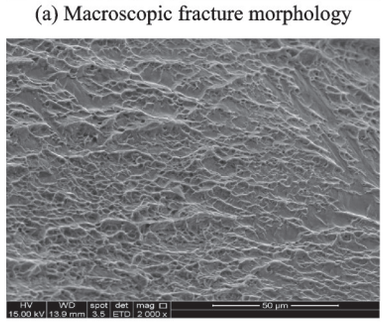

(b) Local magnification of zone 1

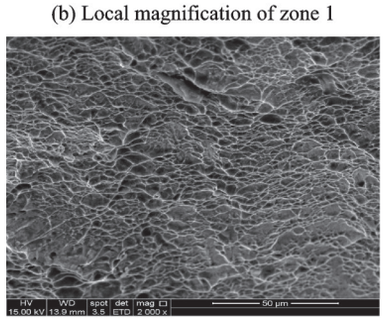

(c) Local magnification of zone 2

Fig.11 Tensile fracture morphology

3 Conclusions

The conclusions were drawn from this research as followed.

(1) Due to the rapid cooling rate, a large amount of acicular martensite is produced in FZ, which is conducive to the improvement of mechanical properties of the joint.

(2) The fusion zone gains the highest microhardness after TIG welding. The tensile strength of the joint is equivalent to that of the base metal, and the fracture mechanism of the joint is mixed ductile-brittle fracture mode.

(3) The content of nitrogen, oxygen and hydrogen of the joint meets the standard, and no obvious surface defects and internal defects are found in TIG joint.

References

[1] KARPAGARAJ A, SIVA S N, SANKARANARAY K, et al. Some studies on mechanical properties and microstructural characterization of automated TIG welding of thin commercially pure titanium sheets[J]. Materials Science & Engineering: A, 2015, 640: 180-189.

[2] RAZAVI G R, MASAELI M, TAHERI M, et al. Investigation gas tungsten arc welding of pure titanium[J]. International Journal of Materials Mechanical Engineering, 2014, 2(1): 1-6.

[3] DENG Q, HONG J, ZENG L, et al. Electron beam welding, laser beam welding and gas tungsten arc welding of titanium sheet[J]. Materials Science & Engineering: A, 2000, 280: 177-181.

[4] WANG J, XU J, WANG C, et al. Microstructure and properties of TiN deposited by pulsed arc cladding on titanium alloy[J]. Welding, 2017, 6: 13-16.

[5] PATNAIK A K, POONDLA N, MENZEMER C C, et al. Understanding the mechanical response of built-up welded beams made from commercially pure titanium and a titanium alloy[J]. Materials Science & Engineering: A, 2014, 590: 390-400.

[6] KUMAR K, MASANTA M, SAHOO S K, et al. Microstructure evolution and metallurgical characteristic of bead-on-plate TIG welding of Ti-6Al-4V alloy[J]. Journal of Materials Processing Tech, 2019, 265: 34-43.

[7] ESMAILY M, MORTAZAVI S N, TODEHFALAH P, et al. Microstructural characterization and formation of α′ martensite phase in Ti-6Al-4V alloy butt joints produced by friction stir and gas tungsten arc welding processes[J]. Materials and Design, 2013, 47: 43-50.

[8] SUNDARESAN S, RAM G J, REDDY G M, et al. Microstructural refinement of weld fusion zones in α-β titanium alloys using pulsed current welding[J]. Materials Science & Engineering: A, 1999, 262(1/2): 88-100.

[9] SU N N, FENG X M, ZANG J J, et al. Microstructure and property of Al-FeCoNiCrAl high entropy alloy composite coating on Ti-6Al-4V during annealing using MA method[J]. Transactions of Nanjing University of Aeronautics and Astronautics, 2020, 37(3): 481-489.

[10] LI L, HE N, XUE H. Chip formation mechanism of deep-hole gun drilling of Ti6Al4V titanium alloy[J]. Transactions of Nanjing University of Aeronautics and Astronautics, 2020, 37(1): 164-174.

[11] CHOI B H, CHOI B K. The effect of welding conditions according to mechanical properties of pure titanium[J]. Journal of Materials Processing Tech, 2008, 201(1/2/3): 526-530.

[12] DANIELSON P, WILSON R, ALMAN D, et al. Microstructure of titanium welds[J]. Journal of Material Structure, 2004, 3: 1-7.

[13] LI X, XIE J, ZHOU Y, et al. Effects of oxygen contamination in the argon shielding gas in laser welding of commercially pure titanium thin sheet[J]. Journal of Material Science, 2005, 40: 3437-3443.

[14] GAO X L, ZHANG L J, LIU J, et al. A comparative study of pulsed Nd: YAG laser welding and TIG welding of thin Ti6Al4V titanium alloy plate[J]. Materials Science & Engineering: A, 2013, 559: 14-21.

[15] CHEN C, FAN C, CAI X, et al. Investigation of formation and microstructure of Ti-6Al-4V weld bead during pulse ultrasound assisted TIG welding[J]. Journal of Manufacturing Processes, 2019, 46: 241-247.

Acknowledgement This work was supported by the Priority Academic Program Development of Jiangsu Higher Education Institution and Beijing Institute of Aeronautical Materials (No.KZ82171509).

Authors Mr. **JIANG Jian** received the B. S. degree in College of Materials Science and Technology of Nanjing

University of Aeronautics and Astronautics in June 2017. He joined in College of Materials Science and Technology of Nanjing University of Aeronautics and Astronautics in September 2017, where he is a Ph.D. candidate. His major is materials processing engineering and his research focuses on the welding of titanium alloy.

Prof. **SHEN Yifu** received the B. S. degree in Chongqing University, Chongqing, China, in 1988. He received the M.S. and Ph.D. degrees in Institute of Metals, Chinese Academy of Sciences, in 1993 and 1998, respectively. From 1999 to 2003, he was a postdoctoral researcher at Nanjing University of Aeronautics and Astronautics. From 1993 to present, he has been with the College Materials Science and Technology, Nanjing University of Aeronautics and Astronautics. His research has focused on friction stir welding and processing, laser rapid forming and metal surface engineering.

Author contributions Prof. **SHEN Yifu** designed the study. Mr. **JIANG Jian** performed the experiments and wrote the manuscript. Mr. **ZHANG Mingjie** reviewed the manuscript. Ms. **QI Lichun** contributed to background of the study. Mr. **CHEN Wenhua** manufactured the samples. All authors commented on the manuscript draft and approved the submission.

Competing interests The authors declare no competing interests.

(Production Editor: XU Chengting)

TC2钛合金TIG焊接头组织性能研究及质量检测

江 剑[1], 齐立春[2], 张明杰[2], 陈文华[1], 沈以赴[1]

(1.南京航空航天大学材料科学与技术学院, 南京 211106, 中国; 2.北京航空材料研究院钛合金研究所, 北京 100095, 中国)

摘要: 对TC2钛合金薄板进行了TIG焊接试验, 获得了成形良好的焊缝。对焊接后接头的断面组织、力学性能、断口形貌及质量检验进行了研究。结果表明, 焊缝组织由大量的针状α′和β块组成。显微硬度曲线表明, 接头熔合区的显微硬度值明显高于热影响区和母材, 母材的显微硬度最低。接头的抗拉强度与母材相当, 断口形貌表明接头的断裂机制为韧-脆混合型断裂。经化学、渗透及X射线检验, 焊缝质量优良。

关键词: TC2钛合金; TIG焊; 显微组织; 力学性能; 质量检验